Taylor & Francis
Taylor & Francis Group

Nuclear Science and Engineering

ISSN: (Print) (Online) Journal homepage: https://www.tandfonline.com/loi/unse20

Evaluation of Kinetic Parameters RSG-GAS Reactor Equilibrium Silicide Core Using Continuous-Energy Monte Carlo Serpent 2 Code

Surian Pinem, Liem Peng Hong, Wahid Luthfi, Tukiran Surbakti & Donny Hartanto

To cite this article: Surian Pinem, Liem Peng Hong, Wahid Luthfi, Tukiran Surbakti & Donny Hartanto (22 Jan 2024): Evaluation of Kinetic Parameters RSG-GAS Reactor Equilibrium Silicide Core Using Continuous-Energy Monte Carlo Serpent 2 Code, Nuclear Science and Engineering, DOI: 10.1080/00295639.2023.2284433

To link to this article: https://doi.org/10.1080/00295639.2023.2284433

Published online: 22 Jan 2024.

NUCLEAR SCIENCE AND ENGINEERING

DOI: https://doi.org/10.1080/00295639.2023.2284433

Evaluation of Kinetic Parameters RSG-GAS Reactor Equilibrium Silicide Core Using Continuous-Energy Monte Carlo Serpent 2 Code

Surian Pinem,[a*] Liem Peng Hong,[b,c] Wahid Luthfi,[a] Tukiran Surbakti,[a] and Donny Hartanto[d]

[a]*National Research and Innovation Agency (BRIN), Research Organization for Nuclear Energy, Research Center for Nuclear Reactor Technology, 80th Building of KST B.J. Habibie (PUSPIPTEK) Serpong, South Tangerang, Banten 15310, Indonesia*

[b]*Tokyo City University, Graduate School of Engineering, Cooperative Major in Nuclear Energy, 1-28-1, Tamazutsumi, Setagaya, Tokyo, Japan*

[c]*Nippon Advanced Information Service, (NAIS Co., Inc.), Scientific Computational Division, 416 Muramatsu, Tokaimura, Ibaraki, Japan*

[d]*Oak Ridge National Laboratory, One Bethel Valley Road, Oak Ridge, Tennessee 37830*

Received September 4, 2023
Accepted for Publication November 9, 2023

Abstract — *The purpose of this study is to determine the kinetic parameters of the RSG-GAS equilibrium core. The calculated kinetic parameters are the effective delayed neutron fraction β_{eff}, the neutron generation time Λ, and the prompt neutron lifetime ℓ since they are related to the safety of nuclear operations. The kinetic parameters were calculated using the Serpent 2 code with the ENDF/B-VII.1 and ENDF/B-VIII.0 nuclear data libraries. Calculations were performed using various adjoint-weighted methods such as Meulekamp's method, Nauchi's method, the Iterated Fission Probability method, and the Perturbation Technique. The calculated results of the six-group delayed neutron fraction by the Meulekamp and the IFP methods showed no significant difference. Choosing the IFP method as the reference, the maximum difference for β_{eff} (694 pcm) is 0.73%, and the maximum difference for Λ and ℓ is 1.89%. The calculated kinetic parameters with ENDF/B-VII.1 and ENDF/B-VIII.0 are quite close, with a maximum difference of 0.9%. The sensitivity analysis results indicate several nuclides and reaction types that dominantly affect the β_{eff} and Λ. The results of the kinetic parameter calculations can be used for the safety analysis of the RSG-GAS equilibrium core.*

Keywords — *Kinetic parameters, RSG-GAS, equilibrium core, Serpent 2, ENDF/B-VII.1, ENDF/B-VIII.0.*

Note — *Some figures may be in color only in the electronic version.*

I. INTRODUCTION

The RSG-GAS reactor is an open pool–type multipurpose research reactor with a nominal thermal power of 30 MW. The reactor uses light water as a coolant and moderator and also beryllium as a reflector. The fuel used in the RSG-GAS reactor was Material Testing Reactor (MTR)–type oxide fuel (U_3O_8-Al) initially, which was later converted to silicide fuel (U_3Si_2-Al) with the same dimension, uranium density, and enriched uranium. The reactor achieved its first criticality in 1987,[1] and in 1999, the core conversion program from oxide fuel (U_3O_8-Al) to silicide fuel (U_3Si_2-Al) was carried out to improve reactor performance. Silicide fuel (U_3Si_2-Al) can be used with higher-density uranium loading to extend the operating cycle of the reactor.[2] The new equilibrium

*E-mail: suri001@brin.go.id

silicide core was proposed and designed by Liem et al.[3] while the transition core strategies from oxide to silicide were investigated and established by Liem and Sembiring.[4]

Kinetic parameters are essential for the safety of reactor operation because they relate to the calculation of reactivity values and transient analysis of the reactor core.[5–8] The kinetic parameters also depend on the core burnup, so it is necessary to calculate the RSG-GAS equilibrium core kinetic parameter. Some of the kinetic parameters used so far in RSG-GAS were provided by the vendor, Interatom, and that was for the oxide fuel of RSG-GAS. The kinetic parameters of RSG-GAS's first working core were evaluated[9]; however, after the core conversion to silicide fuel, the kinetic parameters were not evaluated, and the present work tries to provide them. It is expected that the calculated kinetic parameters of RSG-GAS are also needed during the future validation experiments.

The silicide equilibrium core configuration chosen in this calculation comprises the 88th and 89th cores since the burnup distributions were measured for the 88th core and the calculation results are in good agreement with the measured results.[10,11] The calculation of burnup fraction, excess reactivity, and control rod worth was also carried out, and the results are also close to the experimental results.[12,13] In these calculations, beryllium impurity after operating until the 88th core was also considered.

Serpent 2 is a general-purpose, three-dimensional, and continuous-energy particle code based on the Monte Carlo transport method.[14] This code has the advantage of solving problems of complex reactor core geometries using a continuous-energy nuclear data library. Serpent 2 also was developed with capabilities to calculate point-kinetics parameters such as delayed neutron fractions and neutron generation time. Various methods of calculating adjoint-weighted point-kinetics parameters are implemented on Serpent 2 such as the Iterated Fission Probability (IFP) method; the Perturbation Technique; and methods by Meulekamp, Nauchi, and Kameyama.[15] This paper will evaluate kinetic parameters using the Serpent 2 code with Meulekamp's method, Nauchi's method, the IFP method, and the Perturbation Technique.

Calculations were carried out using the nuclear data libraries ENDF/B-VII.1 and ENDF/B-VIII.0.[16,17] The use of several methods and new cross-sectional data libraries is essential to obtain accurate results. The calculated kinetic parameters are delayed neutron fraction, either its effective delayed neutron fraction β_{eff} or six-group delayed neutron fraction β_i followed by its corresponding delayed neutron precursor decay constant λ_i, the average neutron lifetime ℓ, and the neutron generation time Λ. The effective delayed neutron fraction β_{eff} is also calculated in one operating cycle of RSG-GAS, the 88th core, to determine its changes during burnup.

II. RSG-GAS EQUILIBRIUM SILICIDE CORE

The equilibrium core of the RSG-GAS reactor consists of 40 standard fuel elements (FEs) and 8 control elements (CEs) and is surrounded by beryllium as a reflector. The RSG-GAS FE is composed of 21 U_3Si_2-Al fuel plates with 19.75 wt% enrichment and uranium density of 2.96 g/cm^3 U with 250 g of nominal ^{235}U mass in each FE. The RSG-GAS equilibrium core data are shown in Table I. Each fuel plate was mounted on support parts of the fuel assembly, so light water (H_2O) could pass between each plate as a neutron moderator and coolant. The cross-sectional dimensions of one FE are 8.1 cm long and 7.71 cm wide, with the left and right fuel support having a length of 8.05 cm and a width of 0.45 cm, as depicted in Fig. 1. The CE has the same cross-sectional size as the FE. However, the three outer plates on each side are replaced by two pairs of control guide plates, into which the absorber blades are inserted. So, the number of CEs is only 15 fuel plates, as depicted in Fig. 2. The absorber on the CE is made of Ag-In-Cd with a weight ratio of 80%-15%-5%.

The reactor core has a central irradiation position that occupies 2×2 grid positions and an irradiation position that occupies another four different places. In addition, there are five rabbit system facilities; one is pneumatic, and the rest are hydraulic. Beryllium reflector elements occupy the remaining 37 grid positions, with seven beryllium reflector elements having 50-mm-diameter holes used as irradiation facilities and filled with beryllium when not in use. The equilibrium core of the RSG-GAS reactor with all irradiation facilities within the core is shown in Fig. 3.

III. METHODOLOGY

III.A. Kinetic Parameters

Solving reactor dynamics problems using point kinetics needs kinetic parameters such as effective delayed neutron fraction β_{eff}, neutron generation time Λ, and prompt neutron lifetime ℓ. A delayed neutron fraction is used to show a fraction of delayed neutrons to the whole neutron population being produced in a nuclear reactor. The prompt neutron lifetime is the average age of a neutron from being born from

TABLE I

Reactor Main Design Data of RSG GAS (Silicide Core)*

General	
Reactor type	Pool type
Fuel element type	Low enriched uranium silicide MTR
Cooling system	Forced convection downflow
Moderator and coolant	H_2O
Reflector	Be and H_2O
Nominal power [MW(thermal)]	30
Core characteristics	
Number of FEs	40
Number of CEs	8
Number of fork-type absorbers (pairs)	8
Nominal cycle length (effective full power day)	25
Average burnup at BOC (percent loss of ^{235}U)	23.3
Average burnup at EOC (percent loss of ^{235}U)	31.3
Average discharge burnup at EOC (percent loss of ^{235}U)	53.7
Fuel/CEs	
Fuel/CE dimension (mm)	77.1 × 81 × 600
Fuel plate thickness (mm)	1.3
Coolant channel width (mm)	2.55
Number of plates per FE	21
Number of plates per CE	15
Fuel plate clad material	AlMg2
Fuel plate clad thickness (mm)	0.38
Fuel meat dimension (mm)	0.54 × 62.75 × 600
Fuel meat material	U_3Si_2Al
^{235}U enrichment (wt%)	19.75
Uranium density in meat (g/cm^3)	2.96
^{235}U loading per FE (g)	250
^{235}U loading per CE (g)	178.6
Absorber meat material	Ag-In-Cd
Absorber thickness (mm)	3.38
Absorber clad material	SUS-321
Absorber clad thickness	0.85

*Ref.[1].

a fission reaction until it finally induces fissions with fuel, undergoes a capture reaction, or escapes from the reactor core. On the other hand, the neutron generation time (neutron lifetime) is the average age of a neutron in the reactor core from being produced until it finally reacts with the reactor components or leaves the reactor core.

Delayed neutrons differ from prompt neutrons being produced by fission reactions in the way that delayed neutrons are produced by radionuclide-producing neutrons during their decay process. These radionuclides or isotopes are called the delayed neutron precursor, and their half-life has a delayed effect on the neutron being produced. Delayed neutrons in a nuclear reactor are created from fission products emitting neutrons through radioactive decay, which leads to delayed neutron intensity that changes through time. Some fission products like ^{87}Br with a half-life of 55.65 s decay into ^{86}Kr (2.52%), and ^{137}I with a half-life of 24.13 s decays into ^{136}Xe (7.14%). Both mentioned isotopes decay by (β^-,n) reaction, emitting a neutron, and both are considered as delayed neutron precursors. Isotopes that are in a highly excited state also allow them to eject a neutron during their decay. The delayed neutron fractions of ^{235}U and ^{239}Pu are 650 and 210 pcm, respectively.[18] Since the delayed neutron precursor half-life will affect the delayed neutron intensity as a function of time, in general, there are six groups of

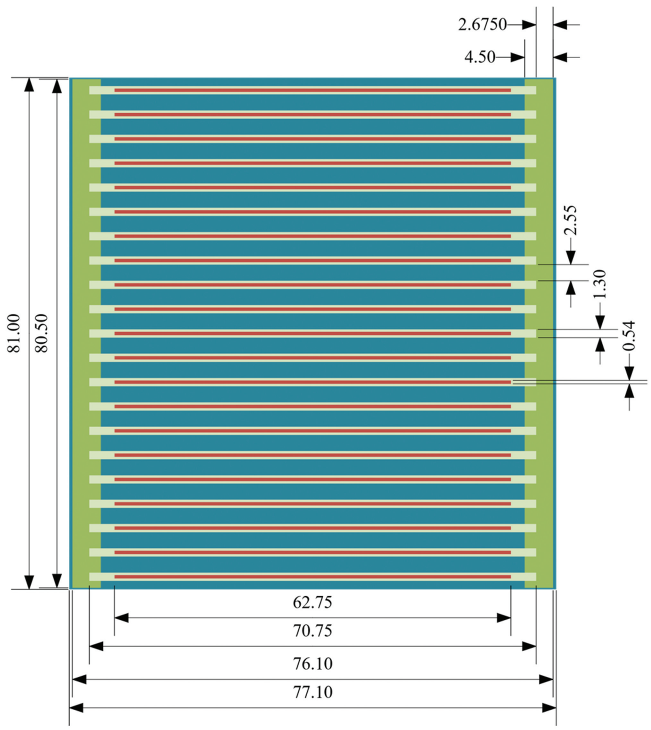

Fig. 1. RSG GAS standard FE (in units of millimeters).[1]

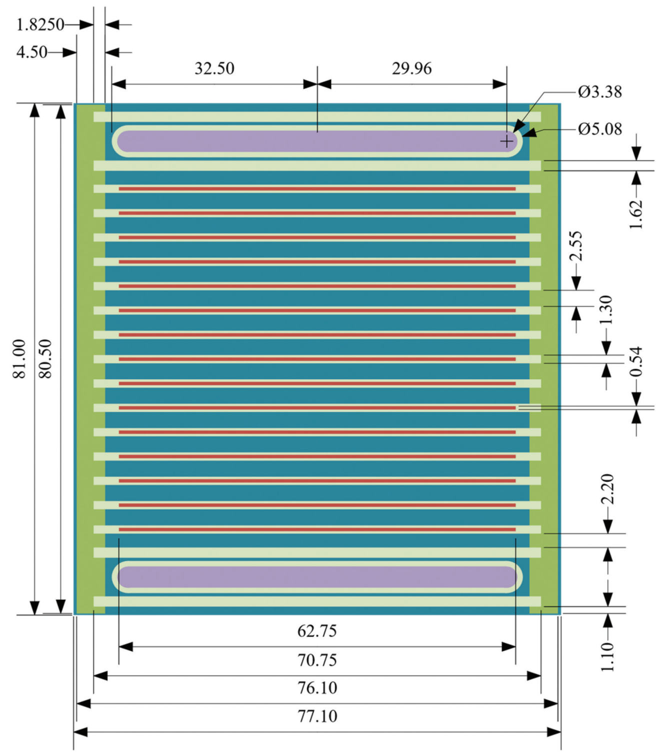

Fig. 2. RSG GAS control FE with absorber blades inserted (in units of millimeters).[1]

delayed neutrons. Although delayed neutrons make up only around 1% of the neutron population in the reactor core, they are important for controlling a nuclear reactor.

III.A.1. Meulekamp-Spriggs (k-Ratio)

In general, the effective delayed neutron fraction β_{eff} or the ratio of the delayed neutron to the total neutron generated on each fission could be written as

$$\beta_{eff} = \frac{S_{delayed}}{S_{total}} \quad . \tag{1}$$

But, there are various approximations regarding how to compute these parameters. Meulekamp used the ratio of fission induced by delayed neutrons to all fission induced by delayed and prompt neutrons to compute β_{eff}.[19] This led to some modifications to the β_{eff} equation:

$$\beta_{eff} = \frac{P_{d,eff}}{P_{eff}} = \frac{\int \phi^{+}(\vec{r},\Omega',E') \int \chi_d(E')\nu_d(E')\Sigma_f(\vec{r},E') \times \phi(\vec{r},\Omega,E)dEd\Omega d\vec{r}d\Omega' dE'}{\int \phi^{+}(\vec{r},\Omega',E') \int \chi(E')\nu(E')\Sigma_f(\vec{r},E') \times \phi(\vec{r},\Omega,E)dEd\Omega d\vec{r}d\Omega' dE'} \quad , \tag{2}$$

where

$\phi(\vec{r},\Omega,E)$ = neutron flux

$\phi^{+}(\vec{r},\Omega',E')$ = adjoint neutron flux

$\Sigma_f(\vec{r},E')$ = macroscopic cross section for fission reaction probability

$\chi(E')$ = fission neutron energy spectrum

$\nu(E')$ = total number of fission neutron emissions on each fission

$\chi_d(E')$ = delayed neutron energy spectrum

$\nu_d(E')$ = number of delayed neutron emissions on each fission.

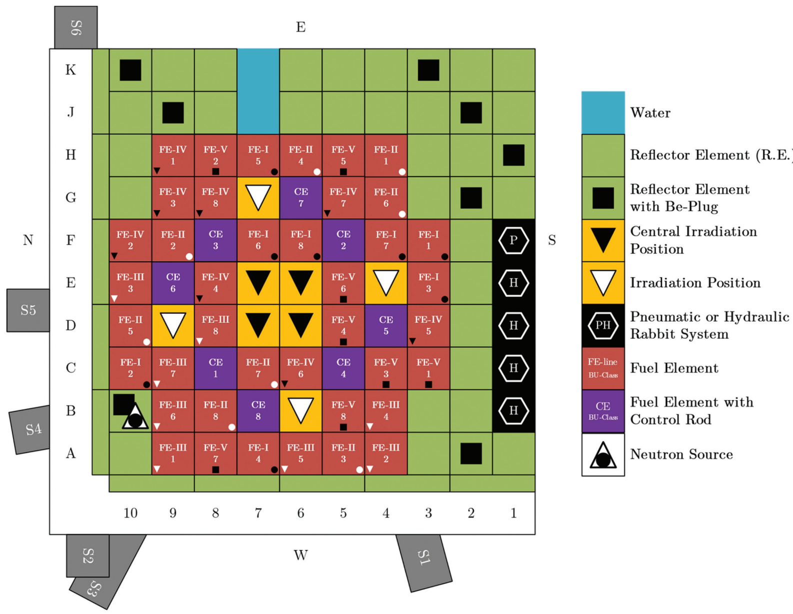

Fig. 3. Equilibrium core of the RSG-GAS reactor.[1]

This equation could be simplified using the operator $\langle f, g\rangle$ to perform an integration over all spatial, angular, and energy variables. By some simplification, this integration could be written into

$$\beta_{eff} = \frac{\langle \phi^+, \chi_d \nu_d \Sigma_f \phi\rangle}{\langle \phi^+, \chi \nu \Sigma_f \phi\rangle} \approx \frac{\langle \chi_d \nu_d\rangle}{\langle \chi \nu\rangle} \quad . \tag{3}$$

Spriggs rewrote the β_{eff} equation, so it focused only on counting the delayed neutron fraction; hence, the k-ratio is then introduced as follows[20]:

$$\beta_{eff} \approx \frac{\langle \chi_d \nu\rangle}{\langle \chi_d \nu\rangle}\frac{\langle \chi_d \nu_d\rangle}{\langle \chi \nu\rangle} \approx \frac{\langle \chi_d \nu_d\rangle}{\langle \chi_d \nu\rangle}\frac{\langle \chi_d \nu\rangle}{\langle \chi \nu\rangle} \approx \beta_0' \frac{\langle \chi_d \nu\rangle}{\langle \chi \nu\rangle} \approx \beta_0' \frac{k_d}{k} \quad . \tag{4}$$

By this equation, β_0' is defined as another delayed neutron fraction by counting the delayed neutron produced by precursors from nuclear data at each fission history, and k_d came from the delayed neutron energy spectrum. On the other hand, the counting delayed neutrons are also proportional to the counting fission induced by the delayed neutrons. This counting process could lead to the very definition of IFP or the number of fissions produced by neutrons that are limited in a critical system.

This happens because in a critical system, the neutron will induce a prompt neutron from fission, some fission products that are precursors for the delayed neutron will decay, and all these neutrons will induce another fission after interacting with the critical system until they reach the limit because it is a critical system. If the system is supercritical, the number of neutrons and fissions will increase on each generation, and the counting process will be hard to follow. Meulekamp implements this approximation by counting fissions induced by delayed neutrons on a generation of the neutron that is used as the seed for the next generation, then called the next fission probability, so it is not necessary to trace all fissions induced by all secondary neutrons on the system.

III.A.2. Chiba (Modified k-Ratio)

In 2009, Chiba proposed some modifications to the implementation of the k-ratio since the Meulekamp approximation is not fully applicable to the various systems mentioned.[21] By assuming that $\nu_p(E')$ is a number of prompt neutron emissions on each fission, $\nu_p = \nu - \nu_d$. With the small amount of delayed neutron fractions and the neutron spectrum that is almost equal to the prompt neutron energy spectrum, the total produced neutrons that are basically formulated into $\chi\nu = \chi_p \nu_p + \chi_d \nu_d$ then could be approximated with $\chi\nu \cong \chi_p \nu_p$. But, since β_{eff} focused on a delayed neutron, Eq. (3) could be modified with the previously mentioned approximation, $\chi_d \nu_d = \chi\nu - \chi_p \nu_p$, so that

$$\begin{aligned}\beta_{eff} &\approx \frac{\langle \chi_d \nu_d\rangle}{\langle \chi \nu\rangle} \approx \frac{\langle \chi\nu - \chi_p \nu_p\rangle}{\langle \chi \nu\rangle} \approx 1 - \frac{\langle \chi_p \nu_p\rangle}{\langle \chi \nu\rangle} \\ &\approx 1 - \frac{k_p}{k} \quad ,\end{aligned} \tag{5}$$

where $\frac{\langle\chi_p\nu_p\rangle}{\langle\chi\nu\rangle}$ leads to a k-ratio of prompt neutron generation at each fission to a total neutron generation. Since k_p is so close to k because the prompt neutrons are constituting almost 99% of the total neutron population, using this equation could lead to higher sensitivity in the calculation of variables k and k_p. From the basic neutron transport equation,

$$L\phi = \frac{1}{k}F\phi \ , \tag{6}$$

where

L = loss term of the neutron transport that includes the absorption reaction and leakage caused by the geometry,

$$L = \Omega \cdot \nabla + \Sigma_t - \int\int \Sigma_s(E',\Omega')dE'd\Omega' \ , \tag{7}$$

F = production term for neutron transport,

$$F = \frac{1}{4\pi}\int\int \chi(E')\nu(E')\Sigma_f(E')dE' \ d\Omega' \ , \tag{8}$$

that applied to its adjoint neutron flux and on a fictitious condition without a delayed neutron,

$$L^+\phi^+ = \frac{1}{k}F^+\phi^+ \text{and } L\phi_p = \frac{1}{k_p}F_p\phi_p \ , \tag{9}$$

where

$$F_p = \frac{1}{4\pi}\int\int \chi_p(E')\nu_p(E')\Sigma_f(E')dE' \ d\Omega' \ , \tag{10}$$

so the $\frac{k_p}{k}$ ratio could be processed by assuming $\phi_p \approx \phi$ for simplification (but could lead to some errors) into

$$\frac{k_p}{k} = \frac{\langle\phi^+, F_p\phi_p\rangle}{\langle\phi^+, F\phi_p\rangle} \approx \frac{\langle\phi^+, F_p\phi\rangle}{\langle\phi^+, F\phi\rangle} \ . \tag{11}$$

Chiba has done some modifications to the k-ratio by considering another fictitious state that uses parameter a as a scaling factor to adjust perturbation from the reference state,

$$L\overline{\phi} = \frac{1}{\overline{k}}\overline{F}\overline{\phi} \ , \tag{12}$$

where

$$\overline{F} = \frac{1}{4\pi}\int\int (\chi\nu + a\chi_d\nu_d)\Sigma_f dE' \ d\Omega' \ , \tag{13}$$

so

$$\beta_{eff} \approx \frac{1}{a}\left(\frac{\overline{k}}{k} - 1\right) \ . \tag{14}$$

III.A.3. Nauchi and Kameyama

Another approximation is by calculating adjoint neutron flux ϕ^+ properly so that it acts as a weighted function to the delayed neutron fraction. Nauchi and Kameyama estimated β_{eff} by taking into account the number of neutrons instead of fissions induced by neutrons, called fission neutrons in the next generation.[22] This approach uses $M(\vec{r},\Omega',E')$ instead of $\phi^+(\vec{r},\Omega',E')$, which has a similar physical meaning as a function of the fission neutron production, so Eq. (3) could be modified to

$$\beta_{eff} = \frac{\langle\phi^+, \chi_d\nu_d\Sigma_f\phi\rangle}{\langle\phi^+, \chi\nu\Sigma_f\phi\rangle} \approx \frac{\langle M, \chi_d\nu_d\Sigma_f\phi\rangle}{\langle M, \chi\nu\Sigma_f\phi\rangle} \ . \tag{15}$$

Nauchi also developed a method to calculate neutron generation time, which came from a modified general equation for Λ:

$$\Lambda = \frac{\int \phi^+(\vec{r},\Omega',E')\frac{1}{\upsilon}\phi(\vec{r},\Omega,E)d\vec{r}d\Omega' dE'}{\int \phi^+(\vec{r},\Omega',E')\frac{1}{4\pi}\int \chi(E')\nu(E')\Sigma_f(E')\phi(\vec{r},\Omega,E)dE'd\vec{r}d\Omega' dE'} \ , \tag{16}$$

where υ is the neutron velocity for corresponding neutron energy, direction, and position. In Monte Carlo, this neutron velocity is important to identify the flight time of a neutron on each track (random walk) within the reactor component. This value, which includes the estimated track length, is evaluated in each neutron collision and absorption. The modification by Nauchi is made by changing the weighted factor of the adjoint neutron flux into M, which is produced by the accounting number of fission neutrons in the next generation:

$$\Lambda = \frac{\langle\phi^+ \frac{1}{\upsilon}\phi\rangle}{\langle\phi^+, F\phi\rangle} \approx \frac{\langle M \frac{1}{\upsilon}\phi\rangle}{\langle M, F\phi\rangle} \ . \tag{17}$$

III.A.4. Iterated Fission Probability

In 2010, Nauchi and Kameyama also developed a new weighting factor to calculate IFP, which then became the name of their new method.[23] Iterated fission probability as defined in Sec. III.A.1 carries the same physical meaning as adjoint neutron flux since the distribution of neutron flux from counting yielded neutrons due to the fission reaction will be proportional to the adjoint neutron flux, which leads to fission probability induced by the neutron at the next generation. This approach will be valid in a critical system when the number of neutrons or fission power generated will achieve a definite level and not increase or decrease exponentially. In this method, IFP was calculated by the number of fission reactions induced by neutrons that could be evaluated from power generated and neutron flux, using pointwise or multigroup cross-section data sets. By calculating IFP $I_{FP}(\vec{r},\Omega',E')$, effective delayed neutron fraction and neutron generation time could be calculated by a similar equation as before with small modification of the weighting factor:

$$\beta_{eff} = \frac{\langle \phi^+, \chi_d \nu_d \Sigma_f \phi \rangle}{\langle \phi^+, \chi \nu \Sigma_f \phi \rangle} \approx \frac{\langle I_{FP}, \chi_d \nu_d \Sigma_f \phi \rangle}{\langle I_{FP}, \chi \nu \Sigma_f \phi \rangle} \tag{18}$$

$$\Lambda = \frac{\langle \phi^+ \frac{1}{\upsilon} \phi \rangle}{\langle \phi^+, F\phi \rangle} \approx \frac{\langle I_{FP} \frac{1}{\upsilon} \phi \rangle}{\langle I_{FP}, F\phi \rangle} \quad . \tag{19}$$

Kiedrowski et al. also developed a power iteration method to calculate the adjoint-weighted tally by using IFP in continuous-energy k-eigenvalue calculation.[24] These tallies are then used to calculate adjoint flux and point-kinetics parameters and to test various cases and to compare those values to reference data.

III.A.5. Verboomen (Perturbation Technique)

Verboomen et al. are developing a perturbation technique to calculate neutron generation time properly for a thermal reactor and fast reactor so it could reduce the difference up to 10%.[25] The Perturbation Technique is implemented by adding a macroscopic capture cross section in each point of the reactor as a perturbation so the reactivity change could be recorded. A perturbed model could be formulated by Eq. (20):

$$L_p \phi_p = \frac{1}{k_p} F_p \phi_p \tag{20}$$

and adjoint equation

$$L^+ \phi^+ = \frac{1}{k^+} F^+ \phi^+ \quad , \tag{21}$$

which could be formulated to the exact perturbation formula for reactivity increment,

$$\Delta\rho = \frac{\langle \phi^+, \left(\frac{1}{k^+}\Delta F - \Delta L\right)\phi_p \rangle}{\langle \phi^+, F_p \phi_p \rangle} \quad , \tag{22}$$

where $\Delta F = F_p - F^+$ and $\Delta L = L_p - L^+$ and by introducing $\frac{c}{\upsilon}$ as a uniform neutron poison as a perturbation, where c is an amplitude constant for homogeneous poison $\frac{1}{\upsilon}$ (υ = neutron speed). Then, the reactivity increment due to perturbation could be formulated to

$$\Delta\rho = \rho_p - \rho^+ = \frac{\langle \phi^+, \frac{c}{\upsilon} \phi_p \rangle}{\langle \phi^+, F^+ \phi_p \rangle} \quad . \tag{23}$$

The derivative of this equation on $c \to 0$ will be equal to the negative of the adjoint neutron generation time or, in general, the neutron generation time equal to the negative value of the reactivity curve slope:

$$\Lambda = -\frac{\Delta\rho}{c} = -\lim_{c \to 0} \frac{1}{c} \frac{\langle \phi^+, \frac{c}{\upsilon} \phi_p \rangle}{\langle \phi^+, F^+ \phi_p \rangle} = \frac{\langle \phi^+, \frac{1}{\upsilon} \phi^+ \rangle}{\langle \phi^+, F^+ \phi^+ \rangle} \quad . \tag{24}$$

III.B. Core Modeling and Calculations

The Serpent core model being used in this study is based on the previous study on the 88th core of RSG-GAS.[9,12] With a total of 48 fuel elements in the core, 5 FEs and 1 CE were fresh fuels. The burnup value for 22 burned FEs came from the burnup measurement, while the remaining 20 burned fuel's burnup values (FE and CE) came from the RSG-GAS report that was calculated using the in-house fuel management code, BATAN-FUEL. Depletion on the 88th core cycle of RSG-GAS was calculated with an average thermal power of 15 MW and generated 627.3375 MWd of thermal energy.

Core thermal power and generated thermal energy are shown in Fig. 4, while control rod position during the 88th core cycle operation is shown in Fig. 5. To achieve about 25 to 30 pcm of the standard deviation of k_{eff}, the depletion calculation was carried out using 50 000 neutron histories per cycle, with a total of 300 cycles, and 100 of them are inactive cycles.

Since all previously mentioned methods of calculating point-kinetics parameters, such as the Meulekamp method,

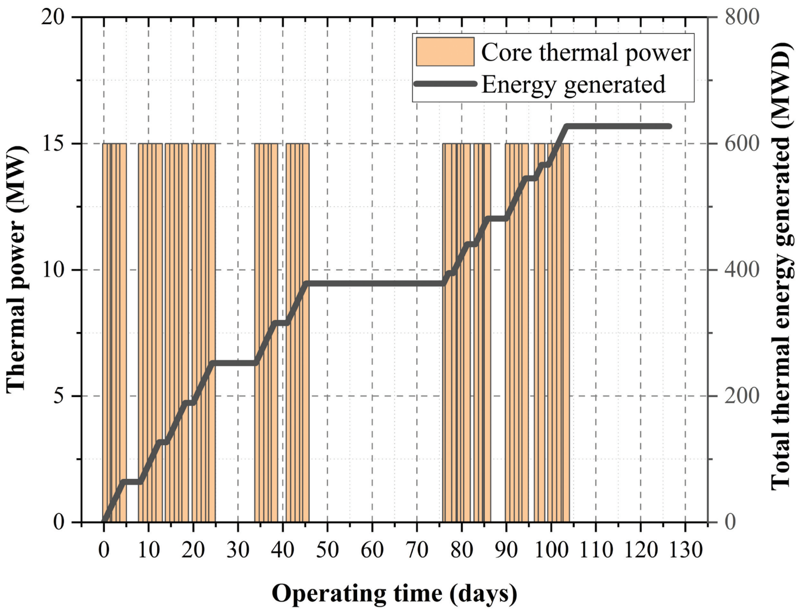

Fig. 4. Core thermal power and energy generated of the 88th core cycle operation.

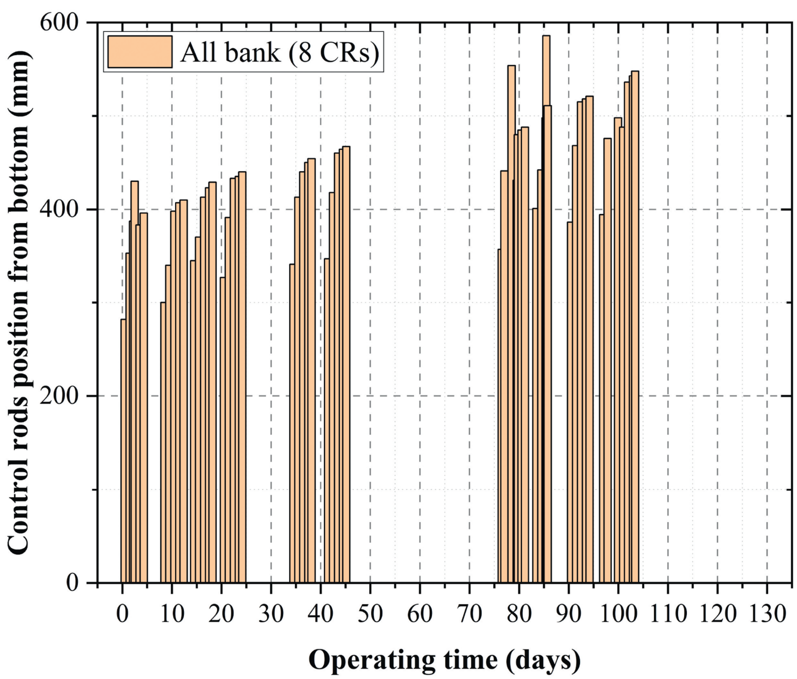

Fig. 5. Control rod position of the 88th core cycle operation.

the Nauchi method, the IFP method, and the Perturbation Technique, have been developed in Serpent,[15] the kinetic parameter calculation was being carried out with all these methods. Kinetic parameters being calculated were the delayed neutron fraction from the beginning of cycle (BOC) of the 88th core burned to the end of cycle (EOC) of the 88th core and at BOC of the 89th core, while the neutron generation time and prompt neutron lifetime were calculated at the BOC of the 88th and 89th cores.

Both ENDF/B-VII.1 and ENDF/B-VIII.0 nuclear data were used in our calculation. Sensitivity analysis was carried out with previously implemented sensitivity calculation capabilities of Serpent based on Generalized Perturbation Theory to propagate nuclear data uncertainties to adjoint-weighted quantities such as delayed neutron fraction, its corresponding decay constant, and prompt neutron lifetime.[26,27] In general, the sensitivity coefficient derived from the sensitivity analysis was defined as the change of the parameter of interest due to a change of other parameters being considered (perturbed), such as microscopic cross sections that were variated in this calculation using different nuclear data sets. For the sensitivity analysis, 252 groups of neutrons for tallying were used with a total of 1200 cycles, 100 of them were inactive cycles, and 200 000 were neutron histories per cycle.

IV. RESULTS AND DISCUSSION

The effective delayed neutron fraction and neutron generation time were calculated by different methods for comparing the consistency of the results obtained. The results of the six-group delayed neutron fraction β_i and delayed neutron decay constant λ_i are shown in Tables II and III. The selected six-group delayed neutron parameters were calculated using Meulekamp's method and the IFP method. Based on the calculation of the six-group delayed neutrons, there was no significant difference between Meulekamp's method and the IFP method, whether it uses ENDF/B-VII.1 and ENDF/B-VIII.0.

The calculated results of β_{eff}, Λ dan ℓ using ENDF/B-VII.1 and ENDF/B-VIII.0 at the BOC of the 88th core are shown in Tables IV and V. Kinetic parameters that were calculated by a different method were compared to the IFP method because this calculation gave good results of kinetic parameter calculation in another MTR-type reactor.[7] Based on the calculation results in Table IV, the β_{eff} value from the Perturbation Technique, compared with the IFP method of 694.01 pcm, gave a maximum difference of 0.77% lower than the IFP method. The value of Λ and ℓ with the IFP method were 78.32 and 79.90 s, respectively, and it also gave a maximum difference of 1.85% with Nauchi's method. There is no significant difference in the value of β_{eff}, Λ, and ℓ in comparison between ENDF/B-VII.1 and ENDF/B-VIII.0.

The calculated results of β_{eff}, Λ dan ℓ using ENDF/B-VII.1 and ENDF/B-VIII.0 on the BOC of the 89th core

TABLE II

Six-Group Delayed Neutron Parameters of 88th Core Using Meulekamp's Method with ENDF/B-VII.1

Group i	Meulekamp's Method		IFP Method	
	β_i (pcm)	λ_i (s^{-1})	β_i (pcm)	λ_i (s^{-1})
1	24.14 ± 0.05	0.013	23.74 ± 0.44	0.013
2	125.02 ± 0.12	0.033	125.81 ± 0.04	0.033
3	119.25 ± 0.11	0.121	121.28 ± 1.03	0.121
4	265.27 ± 0.16	0.303	265.9 6 ± 1.49	0.303
5	110.42 ± 0.11	0.851	110.70 ± 0.98	0.851
6	45.96 ± 0.07	2.856	46.57 ± 0.64	2.856

TABLE III

Six-Group Delayed Neutron Parameters of 88th Core Using Meulekamp's Method with ENDF/B-VIII.0

Group i	Meulekamp's Method		IFP Method	
	β_i (pcm)	λ_i (s^{-1})	β_i (pcm)	λ_i (s^{-1})
1	24.21 ± 0.05	0.013	24.38 ± 0.46	0.013
2	125.38 ± 0.11	0.033	126.03 ± 1.04	0.033
3	119.57 ± 0.11	0.121	121.97 ± 1.02	0.121
4	265.73 ± 0.17	0.303	267.43 ± 1.49	0.303
5	110.74 ± 0.11	0.851	111.33 ± 0.98	0.851
6	46.12 ± 0.07	2.856	46.19 ± 0.64	2.855

TABLE IV

Comparison of Kinetic Parameters Obtained by Different Methods at 88th Core Using ENDF/VII.1

Parameters	Meulekamp's Method	Nauchi's Method	Iterated Fission Probability	Perturbation Technique
Delayed neutron fraction, β_{eff} (pcm)	691.49 ± 0.26 (0.36%)	689.4 1 ± 0.29 (0.66%)	694.01 ± 2.41	694.47 ± 0.17 (−0.77%)
Neutron generation time, Λ (μs)	—	79.77 ± 0.01 (−1.85%)	78.32 ± 0.05	79.15 ± 0.00 (−1.06%)
Prompt neutron lifetime, ℓ (μs)	—	81.14 ± 0.05 (−1.55%)	79.90 ± 0.14	80.75 ± 0.00 (−1.06%)

TABLE V

Comparison of Kinetic Parameters Obtained by Different Methods at 88th Core Using ENDF/VIII.0

Parameters	Meulekamp's Method	Nauchi's Method	Iterated Fission Probability	Perturbation Technique
Delayed neutron fraction, β_{eff} (pcm)	691.75 ± 0.27 (0.65%)	691.32 ± 0.29 (0.71%)	696.25 ± 2.46	695.77 ± 0.19 (0.07%)
Neutron generation time, Λ (μs)	—	79.19 ± 0.01 (−1.84%)	77.76 ± 0.05	78.55 ± 0.00 (0.07%)
Prompt neutron lifetime, ℓ (μs)	—	80.77 ± 0.01 (−1.84%)	79.31 ± 0.05	78.55 ± 0.00 (0.96%)

are shown in Tables VI and VII, respectively. The β_{eff} value with the IFP method was 691.34 pcm, and Nauchi's method gave the maximum difference of 0.41%. The values of Λ dan ℓ with the IFP method were 78.73 and 80.14 s, and the calculated results of each parameter while using ENDF/B-VII.1 and ENDF/B-VIII.0 nuclear data are in good agreement, with a maximum difference of 1.87%. The kinetic parameter values of the 88th and 89th cores also did not change significantly because the dominant fissile material in the reactor core did not change that much at the beginning of each equilibrium core, namely, ^{235}U.

The delayed neutron fraction and the neutron generation time varied with increasing fuel burnup in the reactor core. Changes in kinetic parameters depend on the burnup so it needs to be considered in the calculations. To determine the effect of the fuel fraction on the β_{eff} value, depletion calculations were carried out throughout the operation of the 88th core cycle. The calculation was performed from the BOC value until the EOC of the 88th core, and its results are shown in Fig. 6, with β_{eff} slightly decreasing as the 88th core cycle operated.

It is noticed that there was no significant change in the β_{eff} value during reactor operation since on average,

TABLE VI

Comparison of Kinetic Parameters Obtained by Different Methods at 89th Core Using ENDF/VII.1

Parameters	Meulekamp's Method	Nauchi's Method	Iterated Fission Probability	Perturbation Technique
Delayed neutron fraction, β_{eff} (pcm)	689.40 ± 0.27 (0.28%)	688.51 ± 0.30 (0.41%)	691.34 ± 2.41	693.23 ± 0.197 (−0.27%)
Neutron generation time, Λ (μs)	—	80.12 ± 0.01 (−1.77%)	78.73 ± 0.05	79.51 ± 0.00 (−0.99%)
Prompt neutron lifetime, ℓ (μs)	—	81.55 ± 0.01 (−1.76%)	80.14 ± 0.05	80.93 ± 0.00 (−0.99%)

TABLE VII

Comparison of Kinetic Parameters Obtained by Different Methods at 89th Core Using ENDF/VIII.0

Parameters	Meulekamp's Method	Nauchi's Method	Iterated Fission Probability	Perturbation Technique
Delayed neutron fraction, β_{eff} (pcm)	690.82 ± 0.27 (0.93%)	690.27 ± 0.30 (1.01%)	697.32 ± 2.46	694.76 ± 0.19 (0.37%)
Neutron generation time, Λ (μs)	—	79.59 ± 0.01 (−1.87%)	78.13 ± 0.05	78.99 ± 0.00 (−1.10%)
Prompt neutron lifetime, ℓ (μs)	—	80.88 ± 0.01 (−1.86%)	79.40 ± 0.05	80.27 ± 0.00 (−1.10%)

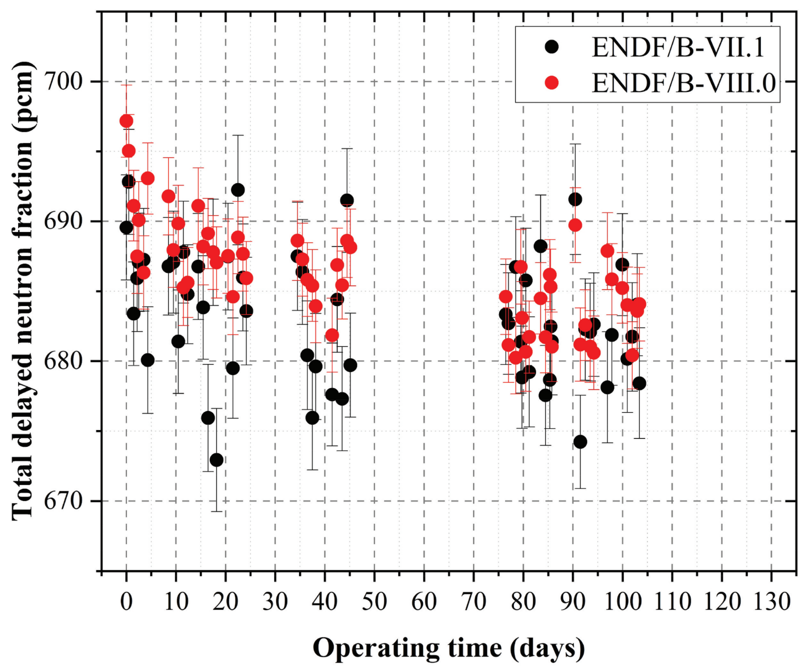

Fig. 6. Total delayed neutron fraction as a function of reactor operation days of 88th core cycle.

each RSG-GAS fuel burnup was increased by around 7% loss of ^{235}U with a maximum fuel burnup of around 56% loss of ^{235}U. So, the increase in ^{239}Pu isotopes that had a lower delayed neutron fraction (around 210 pcm) did not affect the core effective delayed neutron fraction dramatically at the end of the core cycle. Because of no significant changes in the average fuel fraction and fissile material during the RSG-GAS operating cycle, the β_{eff} value fluctuated within a range of 670 to 700 pcm, close to 650 pcm as the β_{eff} value of ^{235}U.[18] Calculation using ENDF/B-VII.1 also showed a slightly stronger fluctuating β_{eff} value than ENDF/B-VIII.0; however, the fluctuation was within or on the same order as the standard deviation of the β_{eff}.

Sensitivity analyses were performed for effective delayed neutron fraction β_{eff} and neutron generation time Λ that were calculated with the ENDF/B-VII.1 and ENDF/B-VIII.0 nuclear data libraries to identify dominant nuclides and reaction types. The β_{eff} sensitivity for each isotope and each nuclear reaction was obtained and sorted according to their absolute values. Then, β_{eff} sensitivity was further classified according to its tendency to increase and decrease when perturbed parameters increased, as shown in Tables VIII and IX, respectively. Both tables show sensitivity with an absolute value of more than 1%, including its isotopes, as well as nuclear reactions being perturbed. The top five contributors that had a tendency to increase β_{eff} were ^{235}U (nu-delayed and

TABLE VIII

Sensitivities of β_{eff} in Increasing Direction*

Nuclide	Perturbation	Sensitivity		ENDF/B-VIII.0 to ENDF/B-VII.1	
		ENDF/B-VII.1	ENDF/B-VIII.0	Deviation	Ratio
^{235}U	Nubar delayed	96.305%	96.512%	0.207%	1.002
^{1}H	Total cross section	9.776%	−15.950%	−25.726%	−1.632
^{1}H	S(α,β) scattering cross section	9.140%	−8.508%	−17.648%	−0.931
^{235}U	Nubar total	2.488%	2.429%	−0.059%	0.976
^{16}O	Total cross section	2.274%	−0.902%	−3.176%	−0.397
^{16}O	Elastic scattering cross section	2.059%	−1.088%	−3.146%	−0.528
^{1}H	Capture cross section	1.760%	0.840%	−0.920%	0.477
^{239}Pu	Nubar delayed	1.469%	1.410%	−0.060%	0.959
^{235}U	Total cross section	1.447%	−1.021%	−2.468%	−0.706
^{238}U	Nubar delayed	1.303%	1.275%	−0.029%	0.978
^{235}U	Fission cross section	1.059%	−0.076%	−1.136%	−0.072

*Absolute value > 1.0%.

TABLE IX

Sensitivities of β_{eff} in Decreasing Direction*

Nuclide	Perturbation	Sensitivity		ENDF/B-VIII.0 to ENDF/B-VII.1	
		ENDF/B-VII.1	ENDF/B-VIII.0	Deviation	Ratio
^{235}U	Nubar prompt	−93.816%	−94.082%	−0.266%	1.003
^{239}Pu	Nubar prompt	−4.200%	−4.098%	0.102%	0.976
^{239}Pu	Nubar total	−2.731%	−2.688%	0.042%	0.984
^{9}Be	*nxn* cross section	−1.553%	−1.246%	0.307%	0.802
^{1}H	Elastic scattering cross section	−1.124%	−8.282%	−7.158%	7.369
^{238}U	Nubar prompt	−1.099%	−1.037%	0.062%	0.944
^{9}Be	S(α,β) scattering cross section	−0.556%	3.005%	3.561%	−5.401
^{9}Be	Total cross section	−0.481%	1.907%	2.388%	−3.966
^{9}Be	Elastic scattering cross section	−0.410%	−1.704%	−1.294%	4.156

*Absolute value > 1.0%.

nu-total), ^{1}H [s(α,β) scattering and total reaction], and ^{16}O (elastic scattering and total reaction), while nu-delayed from ^{235}U dominated with higher than 96% sensitivity. On another hand, the top five contributors with a tendency to decrease the β_{eff} value were ^{235}U (nu-prompt), ^{239}Pu (nu-prompt and nu-total), ^{9}Be [(*n,n*) reaction], and ^{1}H (elastic scattering reaction) while nu-prompt from ^{235}U dominated with higher than 93% sensitivity.

The ENDF/B-VIII.0 to ENDF/B-VII.1 deviation showed the relative difference of ENDF/B-VIII.0 by directly subtracting its value to ENDF/B-VII.1 to emphasize the amount of difference of sensitivity between both nuclear data, while the ratio was used to show that their ratio with a ratio close to unity meant the sensitivities of both nuclear data libraries were almost equal. Since nu-delayed and nu-prompt of ^{235}U were almost equal on both nuclear data and dominated the β_{eff} sensitivity, a small difference on this isotope will affect β_{eff} significantly in both libraries. But, for other isotopes like ^{1}H, their response on s(α,β) scattering and the total reaction was opposed to ENDF/B-VIII.0 by more than −8% sensitive compared to ENDF/B-VII.1 on 9% sensitivity as shown in Table VIII. The elastic scattering of ^{16}O had less sensitive and an opposed response to β_{eff} on ENDF/B-VIII.0 compared to ENDF/B-VII.1. The elastic scattering of ^{1}H also was 7% lower on ENDF/B-VIII.0 compared to ENDF/B-VII.1 as shown in Table IX, with the ^{9}Be (*n,n*) reaction also having a small difference on the sensitivity of β_{eff} from both nuclear data. But, in comparison to nu-delayed and nu-prompt of ^{235}U, their

TABLE X

Sensitivities of Λ in the Increasing Direction*

Nuclide	Perturbation	Sensitivity		ENDF/B-VIII.0 to ENDF/B-VII.1	
		ENDF/B-VII.1	ENDF/B-VIII.0	Deviation	Ratio
^{235}U	Nubar prompt	2.641%	2.602%	−0.039%	0.985
^{9}Be	S(α,β) scattering cross section	2.605%	3.593%	0.988%	1.379
^{9}Be	Elastic scattering cross section	2.448%	2.633%	0.185%	1.076
^{235}U	Nubar total	1.975%	1.943%	−0.031%	0.984
^{9}Be	*nxn* cross section	1.400%	1.382%	−0.019%	0.987

*Absolute value > 1.0%.

TABLE XI

Sensitivities of Λ in Decreasing Direction

Nuclide	Perturbation	Sensitivity		ENDF/B-VIII.0 to ENDF/B-VII.1	
		ENDF/B-VII.1	ENDF/B-VIII.0	Deviation	Ratio
^{1}H	Total cross section	−57.211%	−53.404%	3.807%	0.933
^{235}U	Total cross section	−41.088%	−41.165%	−0.077%	1.002
^{235}U	Fission cross section	−35.147%	−35.005%	0.142%	0.996
^{1}H	Capture cross section	−30.676%	−30.500%	0.177%	0.994
^{1}H	Elastic scattering cross section	−19.312%	−16.622%	2.690%	0.861
^{9}Be	Capture cross section	−8.143%	−8.102%	0.041%	0.995
^{1}H	S(α,β) scattering cross section	−7.223%	−6.283%	0.940%	0.870
^{235}U	Capture cross section	−5.898%	−6.025%	−0.127%	1.022
^{9}Be	Total cross section	−3.091%	−1.877%	1.214%	0.607
^{16}O	Total cross section	−3.005%	−3.089%	−0.085%	1.028
^{16}O	Elastic scattering cross section	−2.921%	−3.008%	−0.087%	1.030
^{239}Pu	Total cross section	−2.042%	−2.046%	−0.005%	1.002
^{239}Pu	Fission cross section	−1.814%	−1.805%	0.009%	0.995
^{239}Pu	Nubar total	−1.324%	−1.287%	0.037%	0.972
^{239}Pu	Nubar prompt	−1.311%	−1.275%	0.036%	0.973
^{238}U	Total cross section	−1.011%	−0.930%	0.082%	0.919

*Absolute value > 1.0%.

contribution to the β_{eff} value might be neglected since the use of ^{1}H, ^{16}O as a moderator (H_2O), and ^{9}Be reflectors was constant with their depletion being omitted during core depletion calculation.

The sensitivity of neutron generation time was also classified according to its tendency to increase and to decrease as shown in Tables X and XI. The top five contributors that tended to increase Λ are ^{235}U (nu-prompt and nu-total) and ^{9}Be [s(α,β) scattering, elastic scatting, and (*n,n*) reaction] with all five contributors having below 4% sensitivity to increase Λ while their value was increased. Meanwhile, the top five contributors that tended to decrease Λ were ^{1}H (total, capture, and elastic scattering reaction), ^{235}U (total and fission reaction), and ^{9}Be (capture reaction), with the total reaction of ^{1}H dominating the sensitivity of Λ by more than 53%. Compared to the sensitivity of β_{eff}, both nuclear data showed a good agreement when calculating the sensitivity of Λ with ENDF/B-VIII.0, which had lower than 4% absolute deviation to ENDF/B-VII.1.

V. CONCLUSION

Several calculations to evaluate the kinetic parameters in the equilibrium core of the RSG-GAS reactor with silicide fuel were carried out using the Serpent code with the ENDF/B-VII.1 and ENDF/B-VIII.0 nuclear data libraries. In this study, the IFP method was used as a reference for comparison with other methods. The values of delayed neutron fraction β_{eff} and prompt neutron lifetime ℓ obtained with the IFP method using ENDF/B-VIII.0 were 696.25 pcm and 79.31 μs, respectively, and there was no significant difference when compared with other methods. The sensitivity of β_{eff} mainly originated from ^{235}U (nu-delayed, nu-total, and nu-prompt), ^{1}H [s(α, β) scattering, elastic scattering reaction, and total reaction], ^{239}Pu (nu-prompt and nu-total), ^{16}O (elastic scattering and total reaction), and ^{9}Be [(n,n) reaction] while nu-delayed and nu-prompt from ^{235}U dominated with higher than 93% sensitivity. On the other hand, the sensitivity of neutron generation time Λ mainly originated from ^{1}H (total, capture, and elastic scattering reaction), ^{9}Be [capture reaction, s(α,β) scattering, elastic scatting, and (n,n) reaction], and ^{235}U (nu-prompt, nu-total, total, and fission reaction), with the total reaction of ^{1}H dominating sensitivity of Λ by more than 53%. The calculated values of the kinetic parameter on the BOC of the 88th and 89th cores did not show a significant difference between ENDF/B-VII.1 and the latest ENDF/B-VIII.0 nuclear data. The results of calculated kinetic parameters could be used for analyzing the safety of the equilibrium core of the RSG-GAS reactor either in steady-state or transient conditions.

Acknowledgments

Thanks are due the head of the Research Center for Nuclear Reactor Technology (PRTRN) Research Organization for Nuclear Energy (ORTN) National Research and Innovation Agency (BRIN) for supporting this research through DIPA 2022. Also Thanks for the support of Department of Mechanical and Nuclear Engineering of the University of Sharjah, United Arab Emirates.

Disclosure Statement

No potential conflict of interest was reported by the author(s).

Funding

This research has been supported by BRIN Indonesia through Rumah Progam Hasil Inovasi Teknologi Nuklir (RP HITN) - Program House for Nuclear Technology Innovation on fiscal year 2022 number B-277/V/TN/4/2022 with its budget came from DIPA-124.01.1.690503/2022.

ORCID

Surian Pinem http://orcid.org/0000-0001-6990-1059
Liem Peng Hong http://orcid.org/0000-0002-0285-4507
Wahid Luthfi http://orcid.org/0000-0002-4499-3433
Tukiran Surbakti http://orcid.org/0000-0002-4081-774X
Donny Hartanto http://orcid.org/0000-0002-9554-1111

References

1. "Multipurpose Reactor G.A. Siwabessy Safety Analysis Report. Rev. 10. Jakarta, Indonesia," RSG-Batan (2011).
2. T. M. SEMBIRING et al., "Neutronic Design of Mixed Oxide-Silicide Cores for the Core Conversion of RSG-GAS Reactor," *At. Indones.*, **27**, *2* (2001).
3. P. H. LIEM et al., "Fuel Management Strategy for the New Equilibrium Silicide Core Design of RSG GAS (MPR-30)," *Nucl. Eng. Des.*, **180**, *3*, 207 (1998); https://doi.org/10.1016/s0029-5493(97)00301-4.
4. P. H. LIEM and T. M. SEMBIRING, "Design of Transition Cores of RSG GAS (MPR-30) with Higher Loading Silicide Fuel," *Nucl. Eng. Des.*, **240**, *6*, 1433 (2010); https://doi.org/10.1016/j.nucengdes.2010.01.028.
5. T. AKYUREK, S. B. SHOAIB, and S. USMAN, "Delayed Fast Neutron as an Indicator of Burn-Up for Nuclear Fuel Elements," *Nucl. Eng. Technol.*, **53**, *10*, 3127 (2021); https://doi.org/10.1016/j.net.2021.04.013.
6. L. SNOJ et al., "Monte Carlo Calculation of Kinetic Parameters for the TRIGA Mark II Research Reactor," *Proc. Int. Conf. Nuclear Energy for New Europe*, Portorož, Slovenia, September 8–11, 2008.
7. M. ARKANI, M. HASSANZADEH, and S. KHAKSHOURNIA, "Calculation of Six-Group Importance Weighted Delayed Neutron Fractions and Prompt Neutron Lifetime of MTR Research Reactors Based on Monte Carlo Method," *Prog. Nucl. Energy*, **88**, 352 (2016); https://doi.org/10.1016/j.pnucene.2015.12.005.
8. T. M. VU et al., "Sensitivity and Uncertainty Analysis of Neutronic and Kinetic Parameters for CERCER and CERMET Fueled ADS Using SERPENT 2 and ENDF/B-VIII.0," *Ann. Nucl. Energy*, **168**, 108912 (2022); https://doi.org/10.1016/j.anucene.2021.108912.
9. D. HARTANTO and P. H. LIEM, "Analysis of the First Core of the Indonesian Multipurpose Research Reactor RSG-GAS Using the Serpent Monte Carlo Code and the ENDF/B-VIII.0 Nuclear Data Library," *Nucl. Eng. Technol.*, **52**, *12*, 2725 (2020); https://doi.org/10.1016/j.net.2020.05.027.

10. S. PINEM et al., "Fuel Element Burnup Measurements for the Equilibrium LEU Silicide RSG GAS (MPR-30) Core Under a New Fuel Management Strategy," *Ann. Nucl. Energy*, **98**, 211 (2016); https://doi.org/10.1016/j.anucene.2016.08.010.

11. T. SURBAKTI et al., "Core Burn-Up Analysis of the RSG-GAS Research Reactor Using Deterministic and Stochastic Methods," *J. Teknol. Sciences Eng.*, **5**, 191 (2022).

12. T. M. SEMBIRING et al., "Analysis of the Excess Reactivity and Control Rod Worth of RSG-GAS Equilibrium Silicide Core Using Continuous-Energy Monte Carlo Serpent2 Code," *Ann. Nucl. Energy*, **154**, 108107 (2021); https://doi.org/10.1016/j.anucene.2020.108107.

13. I. KUNTORO, S. PINEM, and T. SURBAKTI, "Analysis of Control Rod Effect on the Safety Operation Parameter of the RSG-GAS Core," *J. Phys. Conf. Ser.*, **2193**, 012004 (2022); https://doi.org/10.1088/1742-6596/2193/1/012004.

14. J. LEPPÄNEN et al., "The Serpent Monte Carlo Code: Status, Development and Applications in 2013," *Ann. Nucl. Energy*, **82**, 142 (2015); https://doi.org/10.1016/j.anucene.2014.08.024.

15. J. LEPPÄNEN et al., "Calculation of Effective Point Kinetics Parameters in the Serpent 2 Monte Carlo Code," *Ann. Nucl. Energy*, **65**, 272 (2014); https://doi.org/10.1016/j.anucene.2013.10.032.

16. T. M. SEMBIRING and P. H. LIEM, "Accuracy of the ENDF/B-VII.0 Nuclear Data Library on the First Criticality Experiments of the Indonesian Multipurpose Reactor Criticality Experiments of the Indonesian Multipurpose Reactor RSG Gas," *Proc. Int. Conf. Nuclear Data for Science and Technology*, New York, March 2013.

17. D. A. BROWN et al., "ENDF/B-VIII.0: The 8th Major Release of the Nuclear Reaction Data Library with CIELO-Project Cross Sections, New Standards and Thermal Scattering Data," *Nucl. Data Sheets*, **148**, 1 (2018); https://doi.org/10.1016/j.nds.2018.02.001.

18. J. J. DUDERSTADT and L. J. HAMILTON, *Nuclear Reactor Analysis*, John Wiley & Sons, Inc. (1977).

19. R. K. MEULEKAMP and S. C. VAN DER MARCK, "Calculating the Effective Delayed Neutron Fraction with Monte Carlo," *Nucl. Sci. Eng.*, **152**, *2*, 142 (2006); https://doi.org/10.13182/NSE03-107.

20. G. D. SPRIGGS, R. D. BUSCH, and J. M. CAMPBELL, "Calculation of the Delayed Neutron Effectiveness Factor Using Ratios of k-Eigenvalues," *Ann. Nucl. Energy*, **28**, *5*, 477 (2001); https://doi.org/10.1016/S0306-4549(00)00064-5.

21. G. CHIBA, "Calculation of Effective Delayed Neutron Fraction Using a Modified k-Ratio Method," *J. Nucl. Sci. Technol.*, **46**, *5*, 399 (2009); https://doi.org/10.1080/18811248.2007.9711546.

22. Y. NAUCHI and T. KAMEYAMA, "Proposal of Direct Calculation of Kinetic Parameters β_{eff} and Based on Continuous Energy Monte Carlo Method," *J. Nucl. Sci. Technol.*, **42**, *6*, 503 (2005); https://doi.org/10.1080/18811248.2004.9726417.

23. Y. NAUCHI and T. KAMEYAMA, "Development of Calculation Technique for Iterated Fission Probability and Reactor Kinetic Parameters Using Continuous-Energy Monte Carlo Method," *J. Nucl. Sci. Technol.*, **47**, *11*, 977 (2010); https://doi.org/10.1080/18811248.2010.9711662.

24. B. C. KIEDROWSKI, F. B. BROWN, and P. P. H. WILSON, "Adjoint-Weighted Tallies for k-Eigenvalue Calculations with Continuous-Energy Monte Carlo," *Nucl. Sci. Eng.*, **168**, *3*, 226 (2011); https://doi.org/10.13182/NSE10-22.

25. B. VERBOOMEN, W. HAECK, and P. BAETEN, "Monte Carlo Calculation of the Effective Neutron Generation Time," *Ann. Nucl. Energy*, **33**, *10*, 911 (2006); https://doi.org/10.1016/j.anucene.2006.05.001.

26. V. VALTAVIRTA, "Nuclear Data Uncertainty Propagation to Serpent Generated Group and Time Constants," VTT-R-04681-18, VTT (2018); doi:RESEARCH REPORT VTT-R-04681-18.

27. M. AUFIERO et al., "A Collision History-Based Approach to Sensitivity/Perturbation Calculations in the Continuous Energy Monte Carlo Code SERPENT," *Ann. Nucl. Energy*, **85**, 245 (2015); https://doi.org/10.1016/j.anucene.2015.05.008.